International Journal of Innovative Computing, Information and Control
Volume **21**, Number **4**, August **2025**

ICIC International ©2025 ISSN 1349-4198
pp. **987–1002**

DYNAMIC SURFACE ASYMPTOTIC CONTROLLER DESIGN FOR SYNCHRONOUS GENERATORS USING GRAVITATIONAL SEARCH ALGORITHM

Adirak Kanchanaharuthai[1,*], Pinit Ngamsom[2] and Kruawan Wongsurith[3]

[1]Department of Electrical Engineering
[2]Department of Mechanical Engineering
College of Engineering
Rangsit University
52/347 Muang-Ake, Phaholyothin Road, Lak-Hok, Muang, Patumthai 12000, Thailand
pinit.n@rsu.ac.th
[*]Corresponding author: adirak@rsu.ac.th

[3]Faculty of Engineering
Kasem Bundit University
60 Romklao Road, Minburi District, Bangkok 10510, Thailand
kruawan.kru@kbu.ac.th

Received January 2025; revised April 2025

Abstract. *This paper presents a nonlinear state feedback control method designed to stabilize a dual-excited and steam-valving system in synchronous generators. The proposed approach integrates a dynamic surface asymptotic strategy with a gravitational search algorithm to optimize control parameters, significantly improving transient stability, enhancing system frequency regulation, and accelerating convergence. A key innovation of this work is the automated parameter tuning via the gravitational search algorithm, which reduces iteration times while ensuring optimal control performance. Numerical simulations validate the superiority of the proposed method over traditional techniques such as backstepping and immersion-invariance control, demonstrating improved dynamic performance, faster oscillation damping, and enhanced overall system stability.*
Keywords: Dual excitation and steam-valving system, Transient stability enhancement, Dynamic surface asymptotic control, Backstepping control, Gravitational search algorithm

1. **Introduction.** Stabilizing Synchronous Generators (SGs) is a well-recognized challenge in power system stability and operations, primarily due to the frequent disturbances encountered in power networks. As a result, designing nonlinear controllers to stabilize the closed-loop dynamics of nonlinear power systems has become a significant area of research. Two primary methods have been developed to address this challenge while simultaneously achieving control objectives: excitation control schemes [1, 2, 3, 4] and steam-valving control schemes [5, 6, 7].

More recently, combining excitation control with steam-valving control has proven to be a promising and effective solution for enhancing the stability of SGs while optimizing power system operations. This coordinated approach has attracted considerable attention in the power engineering field [8, 9, 10, 11]. For example, a variable structure control strategy that integrates single-excitation and steam-valving control was introduced in [8], utilizing differential geometry and variable structure control theories to deliver robust performance

DOI: 10.24507/ijicic.21.04.987

and dynamic stability. Similarly, nonlinear single-excitation control combined with steam-valving control has been developed using the Hamiltonian function methodology [9, 10], enabling the system to attenuate disturbances and address unknown parameters. Building on these efforts, a robust adaptive single-excitation and steam-valving control strategy [11] was proposed, offering additional flexibility to achieve improved control performance. Most of these studies assume the d-axis field voltage remains constant while focusing on controlling the q-axis field voltage to achieve the desired outcomes. However, using both the d-axis and q-axis field voltages – a method referred to as dual-excitation – offers increased flexibility. With dual-excitation, each field voltage can be independently adjusted, resulting in enhanced stability and improved achievement of control objectives.

To further improve power system stability and transient response, both linear and nonlinear controllers for dual-excited synchronous generators have been developed [12, 13]. Despite this progress, the coordination of dual-excitation and steam-valving control has received limited attention compared to single-excitation and steam-valving approaches. In [14], a coordinated passivation technique was employed to enhance the stability of Single-Machine Infinite Bus (SMIB) systems, demonstrating better dynamic performance than feedback linearization methods. Sliding mode control techniques have also been utilized to design dual-excited and steam-valving controllers for SGs under both matched and mismatched perturbations [15, 16]. These controllers effectively managed mismatched perturbations while improving certain aspects of power quality. Moreover, a nonlinear control algorithm for power systems with dual-excitation and steam-valving control was proposed using the Immersion and Invariance (I&I) strategy [17, 18]. This method significantly enhanced system stability, voltage regulation, and transient behavior in SMIB systems, ensuring power angle stability as well as frequency and voltage regulation. The resulting closed-loop system exhibited transient and asymptotic stability. However, despite its effectiveness, the I&I-based approach has certain limitations that warrant further investigation. A backstepping sliding mode controller [19] was proposed to improve dynamic performance and transient stability while being easier to implement compared to other advanced nonlinear control strategies. A nonlinear disturbance observer-based backstepping control [20] was developed to offer significant improvements over conventional techniques for stabilizing synchronous generators. The method effectively handles external disturbances, improves transient dynamics, and ensures system stability. However, these control laws have various limitations. Backstepping control suffers from a complexity explosion due to repeated differentiation, making it computationally intensive, and it requires precise parameter tuning while lacking robustness against large disturbances. Immersion and Invariance (I&I) control, though effective, is complex to design, sensitive to external disturbances, and may have slow transient responses. Sliding Mode Control (SMC) is limited by chattering effects that can damage actuators, sensitivity to mismatched perturbations, and dependence on proper tuning of parameters. Feedback linearization heavily relies on an accurate system model, making it less robust to uncertainties, and becomes computationally challenging for higher-order systems.

This paper employs a Dynamic Surface Asymptotic Control (DSAC) approach [21] to design the controller, eliminating the need for analytical differentiation of virtual control functions. A key challenge in DSAC lies in selecting appropriate control parameters that stabilize the system while ensuring optimal dynamic performance. Traditional nonlinear control methods, such as backstepping, sliding mode control, and immersion and invariance, face inefficiencies in handling nonlinear systems, including slow responses, sensitivity to parameter tuning, and a lack of robustness and adaptability, particularly under dynamic and steady-state conditions. To address these challenges, this study integrates DSAC with the Gravitational Search Algorithm (GSA) [22, 23], which automates control

parameter tuning to enhance stability and improve performance in nonlinear synchronous generators. Unlike backstepping, which suffers from a complexity explosion due to repeated differentiation, DSAC manages nonlinear dynamics efficiently by incorporating a low-pass filter for virtual control differentiation. However, traditional nonlinear controllers still require manual parameter tuning, which can be inefficient and suboptimal. GSA overcomes this limitation by optimizing control gains, improving stability, transient response, and robustness while reducing overshoot and oscillations. Unlike gradient-based methods, GSA does not require derivatives, making it well-suited for tuning DSAC parameters in systems with complex or unknown mathematical models. This synergistic approach enhances trajectory tracking and dynamic adaptability, ensuring the system remains stable under varying conditions. Beyond power systems, it has broader applications in power electronics, robotics, and aerospace, where nonlinear dynamics and adaptive tuning are crucial for maintaining stability and performance.

The objective of the proposed approach is to develop a stabilizing feedback controller that enhances transient stability and regulates frequency in a Single-Machine Infinite Bus (SMIB) power system model. This ensures satisfactory dynamic and steady-state performance. Furthermore, the proposed method outperforms traditional approaches, such as backstepping control and immersion and invariance control, by achieving asymptotic tracking with zero error. Therefore, the primary contributions of this work lie in that (i) This study presents a Gravitational Search Algorithm (GSA) optimization-based dynamic surface asymptotic control method for transient stability enhancement and frequency regulation in an SMIB power system. This approach addresses a problem that has not been previously explored. (ii) Through Lyapunov theory, it is proven that all signals in the closed-loop system remain bounded, and asymptotic tracking is achieved. (iii) The proposed control design is both simple and highly effective, surpassing traditional methods such as backstepping and immersion and invariance control. It achieves improved dynamic performance, including reduced overshoot and faster oscillation damping.

The remainder of this paper is organized as follows. Section 2 briefly presents the dynamic model of a dual-excited and steam-valving system of synchronous generators, along with key lemmas and the problem statement. In Section 3, the controller design and stability analysis are developed. Section 4 provides a brief overview of the GSA optimization process, while Section 5 presents the simulation results. Finally, Section 6 concludes the paper.

2. Power System Model Description and Preliminaries.

2.1. Power system models.

In this subsection, a dynamic model of a synchronous generator with dual-excited and steam-valving controller [17, 18, 19] can be obtained as follows:

$$\begin{cases} \dot{\delta} = \omega - \omega_s, \\ \dot{\omega} = \dfrac{1}{M}\left(P_m - \dfrac{E'_q}{X'_{d\Sigma}}V_\infty \sin\delta - \dfrac{E'_d}{X'_{q\Sigma}}V_\infty \cos\delta - \dfrac{X'_{d\Sigma} - X'_{q\Sigma}}{2X'_{d\Sigma}X'_{q\Sigma}}V_\infty^2 \sin 2\delta - D(\omega - \omega_s)\right), \\ \dot{P}_m = -\dfrac{P_m - P_{me}}{T_{H\Sigma}} + \dfrac{C_H}{T_{H\Sigma}}u_G, \\ \dot{E}'_q = -\dfrac{X_{d\Sigma}}{X'_{d\Sigma}T'_{d0}}E'_q + \dfrac{(X_{d\Sigma} - X'_{d\Sigma})}{X'_{d\Sigma}T'_{d0}}V_\infty \cos\delta + \dfrac{u_{fd}}{T'_{d0}}, \\ \dot{E}'_d = -\dfrac{X_{q\Sigma}}{X'_{q\Sigma}T'_{q0}}E'_d - \dfrac{\left(X_{q\Sigma} - X'_{q\Sigma}\right)}{X'_{q\Sigma}T'_{q0}}V_\infty \sin\delta + \dfrac{u_{fq}}{T'_{q0}}, \end{cases} \tag{1}$$

where δ is the power angle of the generator, ω denotes the relative speed of the generator, $D \geq 0$ is a damping constant, E'_q and E'_d are the q-axis and d-axis internal transient voltages, respectively. X'_d and X'_q are the d-axis and q-axis transient reactances, respectively. ω_s is the synchronous machine speed, $\omega_s = 2\pi f$, H represents the per unit inertial constant, f is the system frequency and $M = 2H/\omega_s$. $X'_{d\Sigma} = X'_d + X_T + X_L$ is the reactance consisting of the direct axis transient reactance of SG, the reactance of the transformer, and the reactance of the transmission line X_L. Similarly, $X_{d\Sigma} = X_d + X_T + X_L$ is identical to $X'_{d\Sigma}$ except that X_d denotes the direct axis reactance of SG. $X'_{q\Sigma}$ and $X_{q\Sigma}$ denote the q-axis reactances similar to d-axis reactance. T'_{d0} and T'_{q0} are the d-axis and q-axis transient open-circuit time constants. u_{fd} and u_{fq} are the d-axis and q-axis field voltage control inputs to be designed, respectively. P_{me} is the initial value of mechanical power, and C_H is the assigned coefficient of high-pressure cylinder. $T_{H\Sigma}$ is the equivalent time constant of steam valve control systems. u_G is the steam-valving control input to be designed. For convenience, let us define new state variables as follows: $x_1 = \delta - \delta_e$, $x_2 = \omega - \omega_s$, $x_3 = P_m - P_{me}$, $x_4 = \frac{E'_q V_\infty \sin(x_1+\delta_e) - E'_{qe} V_\infty \sin\delta_e}{X'_{d\Sigma}} + m(\sin(2(x_1+\delta_e)) - \sin 2\delta_e)$, $x_5 = \frac{E'_d V_\infty \cos(x_1+\delta_e) - E'_d V_\infty \cos\delta_e}{X'_{q\Sigma}}$, where $m = \frac{X'_{d\Sigma} - X'_{q\Sigma}}{2X'_{d\Sigma}X'_{q\Sigma}}$. Subsequently, after differentiating the state variables above, we have the dynamic model of the dual excitation and steam-valving system of synchronous generators can be expressed as an affine nonlinear system as follows:

$$\dot{x} = f(x) + g(x)u(x), \tag{2}$$

where

$$\begin{cases} f(x) = \begin{bmatrix} f_1(x) \\ f_2(x) \\ f_3(x) \\ f_4(x) \\ f_5(x) \end{bmatrix} = \begin{bmatrix} x_2 \\ \frac{1}{M}\left(x_3 - Dx_2 - x_4 - x_5\right), \\ \frac{P_{me} - x_3}{T_{H\Sigma}} \\ \left(-a_q E'_q + b_q \cos(x_1+\delta_e)\right) \frac{V_\infty \sin(x_1+\delta_e)}{X'_{d\Sigma}} \\ \left(-a_d E'_d - b_d \sin(x_1+\delta_e)\right) \frac{V_\infty \cos(x_1+\delta_e)}{X'_{q\Sigma}} \end{bmatrix}, \\ u(x) = \begin{bmatrix} \frac{C_H}{T_{H\Sigma}} u_G \\ \frac{u_{fd}}{T'_{d0}} \\ \frac{u_{fq}}{T'_{q0}} \end{bmatrix} \\ g(x) = \begin{bmatrix} 0 & 0 & 0 \\ 0 & 0 & 0 \\ g_{31}(x) & 0 & 0 \\ 0 & g_{42}(x) & 0 \\ 0 & 0 & g_{53}(x) \end{bmatrix} = \begin{bmatrix} 0 & 0 & 0 \\ 0 & 0 & 0 \\ 1 & 0 & 0 \\ 0 & \frac{V_\infty \sin(x_1+\delta_e)}{X'_{d\Sigma}} & 0 \\ 0 & 0 & \frac{V_\infty \cos(x_1+\delta_e)}{X'_{q\Sigma}} \end{bmatrix}, \end{cases} \tag{3}$$

where $a_q = \frac{X_{d\Sigma}}{X'_{d\Sigma}T'_{d0}}$, $a_d = \frac{X_{q\Sigma}}{X'_{q\Sigma}T'_{q0}}$, $b_q = \frac{(X_{d\Sigma} - X'_{d\Sigma})}{X'_{d\Sigma}T'_{d0}} V_\infty$, $b_d = \frac{(X_{q\Sigma} - X'_{q\Sigma})}{X'_{q\Sigma}T'_{q0}} V_\infty$. The region of operation is defined in the set $\mathcal{D} = \{x \in \mathcal{S} \times \mathbb{R} \times \mathbb{R} \times \mathbb{R} \times \mathbb{R} | 0 < x_1 < \frac{\pi}{2}\}$. The open loop operating equilibrium is denoted by $x_e = [0,\ 0,\ 0,\ 0,\ 0]^T$.

For the sake of simplicity, the power system considering (2)-(3) can be expressed as follows:

$$\begin{cases} \dot{x}_1 = x_2, \\ \dot{x}_2 = \dfrac{1}{M}(x_3 - Dx_2 - x_4 - x_5), \\ \dot{x}_3 = f_3(x) + g_{31}(x)\dfrac{C_H}{T_{H\Sigma}}u_G, \\ \dot{x}_4 = f_4(x) + g_{42}(x)\dfrac{u_{fd}}{T'_{d0}}, \\ \dot{x}_5 = f_5(x) + g_{53}(x)\dfrac{u_{fq}}{T'_{q0}}. \end{cases} \tag{4}$$

The following assumption and lemmas are established in order to satisfy these required objectives above.

Assumption 2.1. *All state variables $x_1, x_2, x_3, x_4, x_5 \in \mathbb{R}$, are assumed to be measurable.*

Lemma 2.1. [24] *If the constants $p > 1$ and $q > 1$ are such that $(p-1)(q-1) = 1$, then for all $\epsilon > 0$ and all $(x, y) \in \mathbb{R}^2$ we have*

$$xy \leq \frac{\epsilon^p}{p}|x|^p + \frac{1}{q\epsilon^q}|y|^q. \tag{5}$$

If choosing $p = q = 2$ and $\epsilon^2 = 2\kappa$, the inequality above becomes $xy \leq \kappa x^2 + \frac{1}{4\kappa}y^2$.

Lemma 2.2. [25] *The following inequality holds for any $\epsilon > 0$ and for any $z \in \mathbb{R}$*

$$0 \leq |z| - \frac{z^2}{\sqrt{z^2 + \epsilon^2}} < \epsilon. \tag{6}$$

Problem statement: This paper focuses on solving the stabilization problem for the system (4). The primary goal is to design a state feedback controller, $u(x)$, utilizing a dynamic surface asymptotic control approach combined with a gravitational search algorithm. The proposed controller aims to improve transient stability, regulate frequency, and ensure that the overall closed-loop system (4) is asymptotically stable, with all signals in the closed-loop dynamics remaining bounded. In the following section, a design procedure is presented that combines the dynamic surface asymptotic strategy with the gravitational search algorithm to develop the desired nonlinear controller.

3. Controller Design and Stability Analysis.

This section derives the control laws required to stabilize the dual-excitation and steam-valving system of synchronous generators. The design process is structured into two subsections. The first subsection presents the development of a dynamic surface asymptotic control law, which eliminates the need for differentiating virtual control functions at each design step, simplifying implementation. The second subsection analyzes the closed-loop system's behavior using Lyapunov stability arguments, demonstrating that the proposed controller ensures both system stability and desired performance specifications.

3.1. Dynamic surface asymptotic control design.

Following the idea reported in [21], the proposed control procedure is developed step by step as follows.

Step 1: First, let us define the first error surface $S_1 = x_1$, the time derivative of S_1 is defined as

$$\dot{S}_1 = \dot{x}_1 = x_2, \tag{7}$$

and then a Lyapunov function candidate is chosen as $V_1 = \frac{1}{2}S_1^2$. Then the time derivative of V_1 along the first subsystem in (2)-(3) becomes

$$\dot{V}_1 = S_1\dot{S}_1 = S_1(x_2 - x_{2d} + x_{2d} - \alpha_1 + \alpha_1) = S_1(S_2 + e_2 + \alpha_1) \tag{8}$$

where $S_2 = x_2 - x_{2d}$ denotes the error surface and $e_2 = x_{2d} - \alpha_1$ is the boundary layer error. In addition, let us introduce a state variable x_{2d} and let α_1 pass through a first-order filter with time constant τ_2 to obtain x_{2d}

$$\begin{cases} \tau_2\dot{x}_{2d} + x_{2d} = \alpha_2 - \dfrac{\tau_2\hat{M}_2^2 e_2}{\sqrt{\left(\hat{M}_2 e_2\right)^2 + \sigma^2(t)}} - \tau_2 S_1, \quad x_{2d}(0) = \alpha_1(0), \\ \dot{x}_{2d} = -\dfrac{e_2}{\tau_2} - \dfrac{\hat{M}_2^2 e_2}{\sqrt{\left(\hat{M}_2 e_2\right)^2 + \sigma^2(t)}} - S_1, \end{cases} \tag{9}$$

where $\hat{M}_2$ denotes the estimation of M_2, which will be mentioned in the next subsection. Additionally, $\sigma(t)$ is a positive, uniform continuous, and bounded function that satisfies two conditions: $\lim_{t\to+\infty}\int_0^t \sigma(\tau)d\tau \le \sigma_1 < +\infty$ and $|\dot{\sigma}(t)| \le \sigma_2 < +\infty$ where σ_1 and σ_2 are positive constants. We assume that α_1 is a virtual control variable corresponding to the first subsystem of (2) to drive S_1 to zero:

$$\alpha_1 = -c_1 S_1, \tag{10}$$

where c_1 is a positive design constant.

Step 2: Let us consider the second surface as follows:

$$S_2 = x_2 - x_{2d}. \tag{11}$$

We choose the Lyapunov function candidate as $V_2 = \frac{1}{2}S_2^2$. By calculating the derivative of V_2, we have

$$\begin{aligned} \dot{V}_2 &= S_2\dot{S}_2 \\ &= S_2\left[\frac{(x_3 - x_{3d} + x_{3d} - \alpha_2 + \alpha_2) - Dx_2 - (x_4 - x_{4d} + x_{4d} - \alpha_3 + \alpha_3)}{M}\right. \\ &\quad \left. - \frac{(x_5 - x_{5d} + x_{5d} - \alpha_4 + \alpha_4)}{M} - \dot{x}_{2d}\right] \\ &= S_2\left[\frac{S_3 + e_3 + \alpha_2 - Dx_2 - (S_4 + e_4 + \alpha_3) - (S_5 + e_5 + \alpha_4)}{M} - \dot{x}_{2d}\right], \end{aligned} \tag{12}$$

where $S_j = x_j - x_{jd}$, $j = 3, 4, 5$ denote the error surfaces and $e_j = x_{jd} - \alpha_{j-1}$ are the boundary layer errors. We choose the virtual control variables α_{j-1} to drive $S_j \to 0$ as follows:

$$\alpha_2 = \frac{M}{3}(-c_2 S_2 + \dot{x}_{2d}), \quad \alpha_3 = \alpha_4 = -\frac{M}{3}(-c_2 S_2 + \dot{x}_{2d}) - \frac{Dx_2}{2}, \tag{13}$$

where c_2 is a positive constant. Once again, let us consider a state variable x_{jd}; therefore, we pass α_{j-1} through the first-order filters, with time constants τ_j to obtain x_{jd}.

$$\begin{aligned} \dot{x}_{3d} &= -\frac{e_3}{\tau_3} - \frac{\hat{M}_3^2 e_3}{\sqrt{(\hat{M}_3 e_3)^2 + \sigma^2(t)}} - \frac{S_2}{M}, \\ \dot{x}_{kd} &= -\frac{e_k}{\tau_k} - \frac{\hat{M}_k^2 e_k}{\sqrt{(\hat{M}_k e_k)^2 + \sigma^2(t)}} + \frac{S_2}{M}, \quad k = 4, 5, \end{aligned} \tag{14}$$

where $\hat{M}_j$ denotes the estimation of M_j, which will be mentioned in the next subsection.

Step 3: Let us define the third, fourth, and fifth surface errors as $S_j = x_j - x_{jd}$. Then, the Lyapunov function candidate is chosen as $V_3 = \frac{1}{2}\sum_{j=3}^{5} S_j^2$. The time derivative of V_3 along the system trajectories turns into

$$\begin{aligned}\dot{V}_3 &= S_3(\dot{x}_3 - \dot{x}_{3d}) + S_4(\dot{x}_4 - \dot{x}_{4d}) + S_5(\dot{x}_5 - \dot{x}_{5d}) \\ &= S_3\left(f_3(x) + g_{31}(x)\frac{C_H}{T_{H\Sigma}}u_G - \dot{x}_{3d}\right) + S_4\left(f_4(x) + g_{42}(x)\frac{u_{fd}}{T'_{d0}} - \dot{x}_{4d}\right) \\ &\quad + S_5\left(f_5(x) + g_{53}(x)\frac{u_{fq}}{T'_{q0}} - \dot{x}_{5d}\right). \end{aligned} \tag{15}$$

Thus, a suitable control law $u(x) = \left[\frac{C_H}{T_{H\Sigma}}u_G, \frac{u_{fd}}{T'_{d0}}, \frac{u_{fq}}{T'_{q0}}\right]^T$ is selected as follows:

$$\frac{C_H}{T_{H\Sigma}}u_G = -\frac{1}{g_{31}(x)}\left(-c_3S_3 - f_3(x) - \frac{e_3}{\tau_3} - \frac{\hat{M}_3^2 e_3}{\sqrt{\left(\hat{M}_3 e_3\right)^2 + \sigma^2(t)}} - \frac{S_2}{M}\right), \tag{16}$$

$$\frac{u_{fd}}{T'_{d0}} = -\frac{1}{g_{42}(x)}\left(-c_4S_4 - f_4(x) - \frac{e_4}{\tau_4} - \frac{\hat{M}_4^2 e_4}{\sqrt{\left(\hat{M}_4 e_4\right)^2 + \sigma^2(t)}} + \frac{S_2}{M}\right), \tag{17}$$

$$\frac{u_{fq}}{T'_{q0}} = -\frac{1}{g_{53}(x)}\left(-c_5S_5 - f_5(x) - \frac{e_5}{\tau_5} - \frac{\hat{M}_5^2 e_5}{\sqrt{\left(\hat{M}_5 e_5\right)^2 + \sigma^2(t)}} + \frac{S_2}{M}\right), \tag{18}$$

where $g_{31}(x) \neq 0$, $g_{42}(x) \neq 0$, $g_{53}(x) \neq 0$, c_3, c_4 and c_5 are positive design parameters.

3.2. **Stability analysis.** In this subsection, the stability analysis for the presented scheme is investigated. The objective of this part is to indicate that all signals of the closed-loop system are bounded. First, consider the time derivative of the surface errors S_i and the boundary layer errors e_j as follows:

$$\begin{cases} \dot{S}_1 = -c_1S_1 + S_2 + e_2, \quad \dot{S}_2 = \dfrac{1}{M}\left(-c_2S_2 + \dfrac{S_3 - S_4 - S_5}{M} + \dfrac{1}{M}(e_3 - e_4 - e_5)\right), \\ \dot{S}_3 = -c_3S_3, \quad \dot{S}_4 = -c_4S_4, \quad \dot{S}_5 = -c_5S_5, \\ \dot{e}_2 = -\dfrac{e_2}{\tau_2} - \dfrac{\hat{M}_2^2 e_2}{\sqrt{\left(\hat{M}_2 e_2\right)^2 + \sigma^2(t)}} - S_1 + B_2(S_1), \\ \dot{e}_3 = -\dfrac{e_3}{\tau_3} - \dfrac{\hat{M}_3^2 e_3}{\sqrt{\left(\hat{M}_3 e_3\right)^2 + \sigma^2(t)}} - \dfrac{S_2}{M} + B_3\left(S_2, e_2, \hat{M}_2, \sigma(t), \dot{\sigma}(t)\right), \\ \dot{e}_k = -\dfrac{e_k}{\tau_k} - \dfrac{\hat{M}_k^2 e_k}{\sqrt{\left(\hat{M}_k e_k\right)^2 + \sigma^2(t)}} + \dfrac{S_k}{M} + B_k\left(S_2, e_2, \hat{M}_2, \sigma(t), \dot{\sigma}(t)\right), \quad k = 4, 5, \end{cases} \tag{19}$$

where $B_2(\cdot)$, $B_3(\cdot)$, $B_4(\cdot)$, and $B_5(\cdot)$ are continuous functions defined as follows:

$$\begin{cases} B_2(\cdot) = -\dot{\alpha}_1 = -\dfrac{\partial \alpha_1}{\partial x_1}\dot{x}_1 \\ B_l(\cdot) = -\dot{\alpha}_{l-1} = -\dfrac{\partial \alpha_{l-1}}{\partial x_1}\dot{x}_1 - \dfrac{\partial \alpha_{l-1}}{\partial x_2}\dot{x}_2 - \dfrac{\partial \alpha_{l-1}}{\partial \hat{M}_2}\dot{\hat{M}}_2 - \dfrac{\partial \alpha_{l-1}}{\partial e_2}\dot{e}_2 - \dfrac{\partial \alpha_{l-1}}{\partial \sigma(t)}\dot{\sigma}(t),\ l = 3,4,5. \end{cases} \tag{20}$$

Therefore, the main result of this work can be summarized in the following theorem.

Theorem 3.1. *Under Assumption 2.1, we consider the closed-loop dynamics consisting of the SMIB power system model (2)-(3), the control laws (16)-(18), and filters (9) and (14). If there exists a set of suitable design parameters c_i and τ_j ($i = 1,2,3,4,5$, $j = 2,3,4,5$) satisfying $\bar{c}_1 = c_1 - \frac{1}{2} > 0$, $\bar{c}_2 = c_2 - \frac{1}{2} - \frac{3}{2M} > 0$, $\bar{c}_3 = c_3 - \frac{1}{2M} > 0$, $\bar{c}_4 = c_4 - \frac{1}{2M} > 0$, $\bar{c}_5 = c_5 - \frac{1}{2M} > 0$, $\frac{1}{\tau_j} > 0$ such that all trajectories of the overall closed-loop dynamics are bounded, and the surface error S_i converges to zero asymptotically.*

Proof: Let us define the following compact set: $\Omega = \{V(t) \le p\}$ and $\sigma(t)$ and $\dot{\sigma}(t)$ are bounded. Additionally, there exist positive constants M_j such that $|B_j(\cdot)| \le M_j$ on Ω. It is observed from (20) that the explicit values of M_j are unknown, which can be estimated by $\hat{M}_j$, $j = 2,3,4,5$. Let us define the Lynapunov function as

$$V = \frac{1}{2}\left(\sum_{i=1}^{5} S_i^2 + \sum_{j=2}^{5}\left(e_j^2 + \frac{\tilde{M}_j^2}{\beta_j}\right)\right), \tag{21}$$

where $\tilde{M}_j = M_j - \hat{M}_j$. The time derivative of V along trajectories (19) is as follows:

$$\begin{aligned} \dot{V} &= \sum_{i=1}^{5} S_i\dot{S}_i + \sum_{j=2}^{5}\left(e_j\dot{e}_j - \frac{\tilde{M}_j\dot{\hat{M}}_j}{\beta_j}\right) \\ &= S_1(-c_1S_1 + S_2 + e_2) - c_3S_3^2 - c_4S_4^2 - c_5S_5^2 \\ &\quad + S_2\left(-c_2S_2 + \frac{S_3 - S_4 - S_5}{M} + \frac{1}{M}(e_3 - e_4 - e_5)\right) \\ &\quad + e_2\left(-\frac{e_2}{\tau_2} - \frac{\hat{M}_2^2 e_2}{\sqrt{\left(\hat{M}_2 e_2\right)^2 + \sigma^2(t)}} - S_1 + B_2(\cdot)\right) \\ &\quad + e_3\left(-\frac{e_3}{\tau_3} - \frac{\hat{M}_3^2 e_3}{\sqrt{\left(\hat{M}_3 e_3\right)^2 + \sigma^2(t)}} - \frac{S_2}{M} + B_3(\cdot)\right) \\ &\quad + \sum_{k=4}^{5} e_k\left(-\frac{e_k}{\tau_k} - \frac{\hat{M}_k^2 e_k}{\sqrt{\left(\hat{M}_k e_k\right)^2 + \sigma^2(t)}} + \frac{S_2}{M} + B_k(\cdot)\right) - \sum_{j=2}^{5}\frac{\tilde{M}_j\dot{\hat{M}}_j}{\beta_j}. \end{aligned} \tag{22}$$

For $i = 1,2,3,4,5$, $j = 2,3,4,5$ and $p > 0$, the set $\Omega := \sum_{i=1}^{5} V_i + \sum_{j=2}^{5}\frac{1}{2}\left(e_j^2 + \frac{\tilde{M}_j^2}{\beta_j}\right) \le p$ is the compact set. According to the property of continuous function, we know that $B_j(\cdot)$ has a bound on Ω, such that $|B_j(\cdot)| \le M_j$, $j = 2,3,4,5$. Based on Lemma 2.1, we have the following inequalities:

$$S_1S_2 \le \frac{S_1^2}{2} + \frac{S_2^2}{2}, \quad \frac{1}{M}S_2S_3 \le \frac{S_2^2}{2M} + \frac{S_3^2}{2M}, \quad -\frac{1}{M}S_2S_4 \le \frac{S_2^2}{2M} + \frac{S_4^2}{2M},$$
$$-\frac{1}{M}S_2S_5 \le \frac{S_2^2}{2M} + \frac{S_5^2}{2M}. \tag{23}$$

From the inequalities above, one has

$$\dot{V} \le -\left(c_1 - \frac{1}{2}\right)S_1^2 - \left(c_2 - \frac{1}{2} - \frac{3}{2M}\right)S_2^2 - \left(c_3 - \frac{1}{2M}\right)S_3^2 - \left(c_4 - \frac{1}{2M}\right)S_4^2$$
$$-\left(c_5 - \frac{1}{2M}\right)S_5^2 - \sum_{j=2}^{5}\left[\frac{e_j^2}{\tau_j} - \frac{\hat{M}_j^2 e_j^2}{\sqrt{\left(\hat{M}_j e_j\right)^2 + \sigma^2(t)}} + M_j|e_j| - \frac{\tilde{M}_j\dot{\hat{M}}_j}{\beta_j}\right]. \tag{24}$$

According to Lemma 2.2, it is straightforward to compute

$$M_j|e_j| = \hat{M}_j|e_j| + \tilde{M}_j|e_j| \le \frac{\hat{M}_j^2 e_j^2}{\sqrt{\left(\hat{M}_j e_j\right)^2 + \sigma^2(t)}} + \sigma(t) + \tilde{M}_j|e_j|. \tag{25}$$

Subsequently, one obtains $\dot{V} \le -\sum_{i=1}^{5}\bar{c}_i S_i^2 - \sum_{j=2}^{5}\frac{e_j^2}{\tau_j} - \sum_{j=2}^{5}\frac{1}{\beta_j}\tilde{M}_j\left(\dot{\hat{M}}_j - \beta_j|e_j|\right) + 4\sigma(t)$. After designing the update laws for $\hat{M}_j$ as $\dot{\hat{M}}_j = \beta_j|e_j|$, we get $\dot{V} \le -\sum_{i=1}^{5}\bar{c}_i S_i^2 - \sum_{j=2}^{5}\frac{e_j^2}{\tau_j} + 4\sigma(t)$. By integrating the expression above over $[0, t]$, we have

$$V(t) \le V(0) - \int_0^t\left(\sum_{i=1}^{5}\bar{c}_i S_i^2 + \sum_{j=2}^{5}\frac{e_j^2}{\tau_j}\right) + 4\int_0^t\sigma(\tau)d\tau \le V(0) + 4\sigma_1. \tag{26}$$

From (26), it implies that S_i, e_j and $\hat{M}_j$ are bounded. This means that by definition x_i, $i = 1, 2, 3, 4, 5$, α_{j-1}, $j = 2, 3, 4, 5$, and u are all bounded. This completes the proof.

It can be observed that the developed controller $u(x)$ is a nonlinear function that is affected by the choice of the control parameters: $\mathbf{y} = [c_1,\ c_2,\ c_3,\ c_4,\ c_5,\ \tau_2,\ \tau_3,\ \tau_4,\ \tau_5,\ \beta_2,\ \beta_3,\ \beta_4, \beta_5]$. The setting of these control parameters or gains is the topic of the next section.

Remark 3.1. *The proposed control law avoids analytical differentiators, relying on gain control, filter parameters, and nonlinear adaptive terms to reduce complexity. Key differences include (i) it is based on nonlinear control theory, independent of operating points, and (ii) it mitigates complexity better than backstepping or immersion methods. Control parameters are determined using the gravitational search algorithm, as detailed next.*

4. **Gravitational Search Algorithm (GSA) Optimization.** The Gravitational Search Algorithm (GSA) [22, 23] is an optimization method inspired by Newtonian gravity, where agents represent solutions and interact as masses under gravitational forces. Heavier masses, representing better solutions, attract lighter ones, guiding the search process toward optimal solutions. The algorithm effectively balances exploration and exploitation through a decaying gravitational constant and reduced agent interactions over time. GSA consistently outperforms methods like Particle Swarm Optimization (PSO), Real Genetic Algorithm (RGA), and Central Force Optimization (CFO) in various scenarios, demonstrating faster convergence and superior results. Its simplicity and adaptability make it particularly effective for solving complex, high-dimensional optimization problems. By modeling optimization as a system where particles interact via gravitational forces, GSA simulates the natural process of objects moving toward each other under gravity to identify optimal solutions. In the power systems, the control parameters $\mathbf{y}$ must be simultaneously

selected to ensure the closed-loop system achieves asymptotic stability and the all signals remain bounded. The goal is to minimize a performance index, or objective function J, such as the Integral of Time-weighted Absolute Error (ITAE), by adjusting the control gains. The problem is formulated as

$$J = \int_0^{\bar{T}} t^2(|\delta - \delta_e| + |\omega - \omega_s|)dt, \tag{27}$$

where $\bar{T}$ denotes the final simulation time. The ITAE is commonly used to evaluate control systems, with a lower value indicating better performance (i.e., faster error reduction and better system stability). The steps of the GSA algorithm are as follows.

1) **Initialization:** Define the optimization problem: Minimize the objective function $J = f(\mathbf{y})$ in (27), where $\mathbf{y} \in \mathbb{R}^{13}$. Set parameters: number of agents N, maximum iterations T, and gravitational constant G_0 (initialized with a high value) and decay rate α. Initialize agents: randomly generate N agents' positions $\mathbf{y}_i$ in the search space, and initialize agents' velocities $\mathbf{v}_i = 0$.
2) **Fitness Calculation:** Evaluate the fitness $J = f(\mathbf{y}_i)$ for each agent i. Compute the mass M_i of each agent: $M_i = \frac{f_i - f_{\text{worst}}}{f_{\text{best}} - f_{\text{worst}}}$ where f_{best} and f_{worst} are the best and worst fitness values in the current population. Then, normalize the masses: $m_i = \frac{M_i}{\sum_{j=1}^{N} M_j}$.
3) **Gravitational Force Calculation:** Compute the gravitational force F_{ij} exerted on agent i by agent j: $F_{ij} = G \cdot \frac{m_i \cdot m_j}{R_{ij} + \epsilon}(\mathbf{y}_j - \mathbf{y}_i)$, where $R_{ij} = \|\mathbf{y}_j - \mathbf{y}_i\|$ is the Euclidean distance. ϵ is a small constant to avoid division by zero. Compute the total force $\mathbf{F}_i$ acting on agent i in all dimensions: $\mathbf{F}_i = \sum_{j=1, j\neq i}^{N} F_{ij}$.
4) **Acceleration and Velocity Update:** Calculate the acceleration $\mathbf{a}_i$ of each agent: $\mathbf{a}_i = \frac{\mathbf{F}_i}{m_i}$. Update the velocity $\mathbf{v}_i$ of each agent: $\mathbf{v}_i = r \cdot \mathbf{v}_i + \mathbf{a}_i$, where r is a random number in $[0, 1]$. Update the position $\mathbf{y}_i$ of each agent: $\mathbf{y}_i = \mathbf{y}_i + \mathbf{v}_i$.
5) **Gravitational Constant Update:** Decrease the gravitational constant G over time: $G = G_0 \cdot e^{-\alpha \cdot t/T}$, where G_0 is the initial gravitational constant, α is a user-defined decay rate, t is the current iteration, and T is the maximum number of iterations.
6) **Termination:** Repeat steps 2) to 5) until the maximum number of iterations T is reached, or a stopping criterion is met (e.g., convergence). Return the best solution $\mathbf{y}_{\text{best}}$ and its fitness $J = f(\mathbf{y}_{\text{best}})$.
7) **Conclusion:** The GSA algorithm iteratively searches for the optimal values of the thirteen controller parameters, enhancing the performance of the power system based on the objective function defined at the beginning.

Remark 4.1. *To configure the Gravitational Search Algorithm (GSA)* [22, 23]*, start with a high G_0 for exploration, decreasing it exponentially to focus on exploitation. Use a higher decay rate α for faster exploitation. Set N based on problem complexity – larger N increases exploration but costs more, while smaller N risks premature convergence. Randomly initialize positions $\mathbf{y}_i$ and small or zero velocities $\mathbf{v}_i$. Use a small ϵ to avoid division by zero and normalize masses to prevent dominance. Add a randomness factor r for exploration, and define stopping criteria (e.g., max iterations or fitness) while fine-tuning parameters if needed.*

Remark 4.2. *As mentioned eariler in the Introduction section, traditional excitation and steam-valving controls enhance transient stability but rely on single-excitation, limiting flexibility and robustness. While combined excitation-steam-valving methods improve stability using nonlinear techniques, they remain complex and focus on single-excitation*

approaches. Dual-excitation control offers greater flexibility, yet its integration with steam-valving is underexplored, and existing nonlinear methods like sliding mode and I&I control suffer from complexity and sensitivity to parameter tuning. To address these gaps, this study proposes a dual-excitation and steam-valving control strategy that independently regulates d-axis and q-axis field voltages for improved stability. By integrating Dynamic Surface Asymptotic Control (DSAC) with the Gravitational Search Algorithm (GSA), the approach eliminates complexity explosion and enables automatic parameter tuning. This enhances adaptability, reduces overshoot, dampens oscillations, and ensures robustness against disturbances and parameter uncertainties more effectively than conventional methods.

Remark 4.3. *Control parameters are selected based on stability, performance, and robustness considerations. Gains are chosen to satisfy Lyapunov stability conditions, ensuring global asymptotic stability, while ITAE minimization optimizes dynamic performance by reducing overshoot, settling time, and steady-state error. To enhance robustness against disturbances, gains are systematically tuned using the Gravitational Search Algorithm (GSA), which automates selection for efficiency. The chosen gains impact system behavior by ensuring global stability, balancing response speed to prevent excessive overshoot, and maintaining robust performance under varying conditions.*

5. **Simulation Results.** In this section, simulation results are given to indicate the effectiveness of the developed strategy. The proposed controller is evaluated via simulations of a Single-Machine Infinite Bus (SMIB) power system consisting of dual-excited and steam-valving control as shown in Figure 1 [17]. The performance of the proposed control scheme is evaluated and verified in computer simulation.

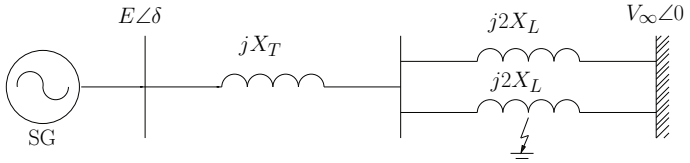

FIGURE 1. A single-line diagram of the SMIB model

The physical parameters (pu.) and initial conditions used for this power system model are the same as those used in [17] as follows: (a) The parameters of dual-excitation and steam-valving system and transmission line: $\omega_s = 2\pi f$ rad/s, $D = 5$, $H = 5$, $f = 60$ Hz, $T'_{d0} = 10$, $T'_{q0} = 4$, $V_\infty = 1\angle 0°$, $X_q = 1.6$, $X'_q = 0.38$, $X_d = 1.6$, $X'_d = 0.23$, $T_{H\Sigma} = 0.4$, $X_T = 0.13$, $X_L = 0.17$, (b) Initial conditions $\delta_e = 0.3445$ rad, $\omega = \omega_s$, $P_{me} = 1.2749$, $E'_{qe} = 1.0703$, $E'_{de} = 0.522$.

Based on the guidelines in [22, 23] for GSA parameter selection, the search space consists of 13 dimensions, with 30 agents (N) employed. The decay rate of the gravitational constant (α) is set to 20, while the initial gravitational constant (G_0) is initialized at 100. The optimization process is constrained to a maximum of 100 iterations (T). The admissible ranges for each controller gain are defined as follows: $10 \leq c_i \leq 200$, $i = 1, 2, 3, 4, 5$, $0.0001 \leq \tau_j \leq 0.01$, and $0.01 \leq \beta_j \leq 1000$, $j = 2, 3, 4, 5$. To minimize the impact of random variations, multiple independent trials were conducted. The final optimized controller values are determined as $c_1 = 143.98$, $c_2 = 171.4172$, $c_3 = 61.45$, $c_4 = 55.89$, $c_5 = 113.66$, $\tau_2 = 0.0021$, $\tau_3 = 0.0068$, $\tau_4 = 0.0080$, $\tau_5 = 0.0039$, $\beta_2 = 562.45$, $\beta_3 = 147.96$, $\beta_4 = 685.18$, $\beta_5 = 629.51$, $\sigma(t) = 0.1e^{-0.01t}$, and $J = 0.0039$.

This study investigates a symmetrical three-phase short circuit occurring at point P on one of the two transmission lines, as depicted in Figure 1. The analysis is organized

into the following stages: (i) the system operates in a steady state before the fault, (ii) a symmetrical three-phase short circuit occurs at $t = 0.5$ seconds, (iii) the fault is cleared by opening the breaker on the affected line at $t = 1.0$ seconds, (iv) the transmission line is fully restored and fault-free at $t = 1.5$ seconds, and (v) the system reaches a steady post-fault state.

The time domain simulations are carried out to investigate the system stability enhancement and the dynamic performance of the designed controller, as given in (16)-(18), in the system in the presence of external disturbances. The control performance of the proposed controller is compared with that of the nonlinear controllers: backstepping controller [24] and immersion and invariance controller [19].

The simulation results are presented and analyzed as follows. Time trajectories of the power angle δ, frequency ω, mechanical power P_m, and the d-axis and q-axis transient internal voltages under the proposed controller and the other controllers are shown in Figures 2 and 3, respectively. Additionally, Figure 4 displays the time histories of the adaptive parameters $\hat{M}_2$, $\hat{M}_3$, $\hat{M}_4$, and $\hat{M}_5$. From these figures, it is evident that the proposed controller successfully achieves the control objectives, even in the presence of a three-phase fault. The results clearly demonstrate that the proposed controller outperforms the other methods by demonstrating superior stability, quicker recovery, and minimal oscillations. In contrast, backstepping and I&I controls exhibit significant oscillations and slower convergence, with I&I performing the weakest overall. This highlights the robustness and efficiency of the proposed control approach. Finally, Figure 4 highlights the time histories of the adaptive parameters, further validating the controller's effectiveness.

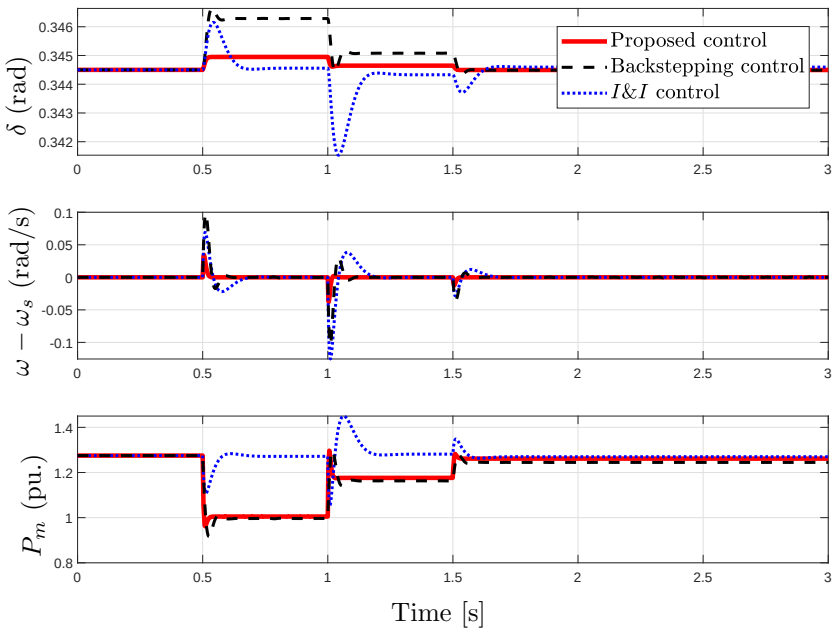

FIGURE 2. Time responses of power angle (δ) (rad), frequency ($\omega - \omega_s$) rad/s and mechanical input (P_m) (pu.)

Table 1 evaluates the performance of different control strategies using the ITAE (Integral of Time-weighted Absolute Error) criterion. While the I&I control strategy shows good performance, its ITAE value is higher than those of both the backstepping method and the proposed approach. The proposed method outperforms the others in minimizing the time-weighted error, highlighting its superior effectiveness in enhancing control system

performance based on this metric. Additionally, Table 2 summarizes the performance of different controllers under a three-phase short circuit disturbance.

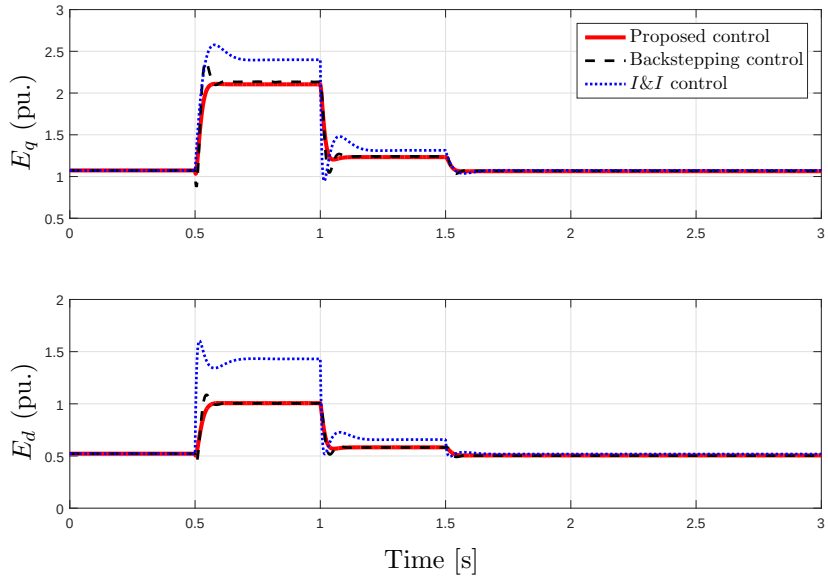

FIGURE 3. Time responses of the q-axis transient internal voltage (E_q) (pu.) and the d-axis transient internal voltage (E_d) (pu.)

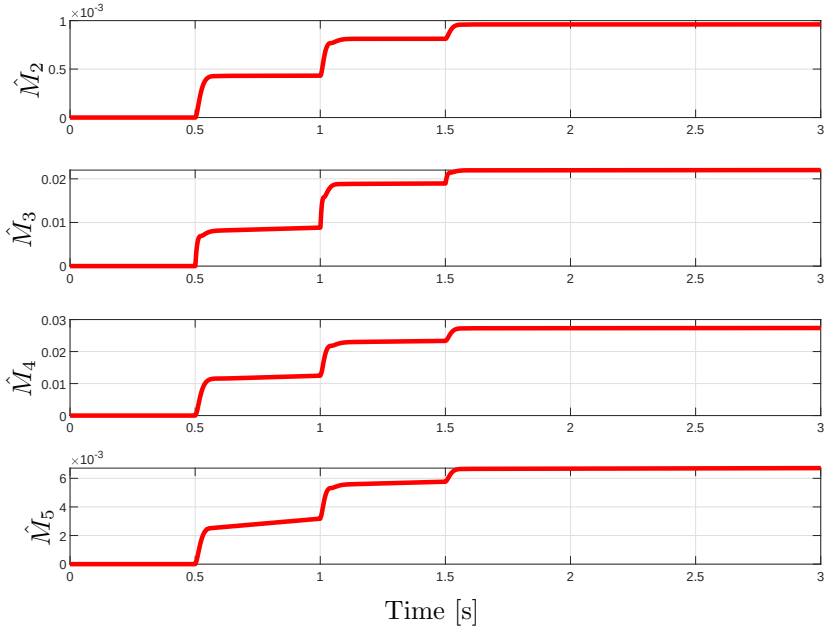

FIGURE 4. Time responses of adaptive parameters $\hat{M}_j$, $j = 2, 3, 4, 5$

TABLE 1. Performance criterion corresponding to the proposed method, backstepping method, and immersion and invariance method

	Proposed control	Backstepping control	I&I control
ITAE	**0.0039**	0.0064	0.0073

TABLE 2. Comparison of power angle response characteristics for different controllers under the three-phase short circuit disturbance

Control method	Peak overshoot (%)	Settling time (s)
Backstepping control	1.45	2.30
I&I control	0.82	2.55
Proposed DSAC + GSA	**0.28**	**1.52**

From Table 2, it is evident that the proposed DSAC + GSA approach significantly reduces settling time while minimizing peak overshoot, indicating superior stability and rapid oscillation attenuation.

In practical applications, achieving a perfectly accurate dynamic model of a system is unattainable. Therefore, it is crucial to evaluate the robustness of the proposed controller against variations in system parameters. One key parameter to consider is the inertia constant H, which is inherently uncertain and difficult to determine precisely. To assess the controller's robustness, the inertia constant H was intentionally varied by $\pm 30\%$ from its nominal value. As illustrated in Figure 5, the proposed scheme continues to deliver stable control performance despite these variations. This indicates that the designed controller remains effective and reliable, demonstrating strong robustness to parameter uncertainty in the system.

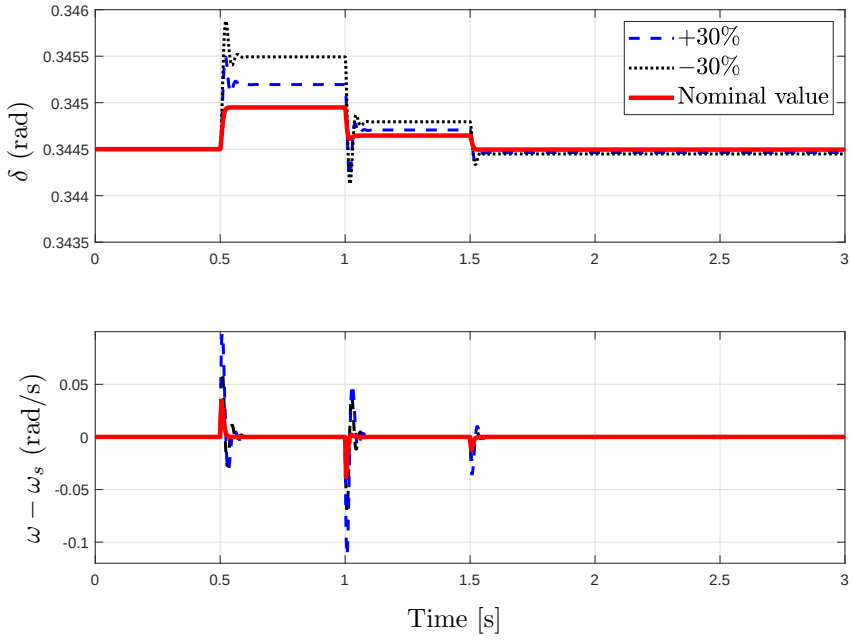

FIGURE 5. Time responses of power angle (δ) (rad), frequency ($\omega - \omega_s$) rad/s under parameter variations of the inertia constant H

The simulation results demonstrate that the proposed dynamic surface asymptotic control method, optimized with the Gravitational Search Algorithm (GSA), offers significant advantages over backstepping and immersion and invariance methods in the SMIB power system. (i) The control law effectively stabilizes the system under disturbances without requiring analytical differentiation, unlike backstepping and immersion and invariance methods. (ii) The proposed strategy ensures faster convergence of the closed-loop dynamics to the desired equilibrium point while exhibiting superior transient performance

by rapidly suppressing oscillations across all time trajectories, even in the presence of substantial disturbances.

6. **Conclusion.** This paper presents a dynamic surface asymptotic control strategy integrated with Gravitational Search Algorithm (GSA) optimization for a dual excitation and steam-valving system of synchronous generators. The proposed method aims to achieve superior dynamic performance, enhance transient stability, and ensure effective frequency regulation. To verify its effectiveness, simulations are conducted using a dynamic model of the dual-excited and steam-valving system. The results reveal that the proposed control approach significantly improves transient performance and surpasses backstepping and immersion and invariance controllers. Comparative analyses highlight the controller's capability to rapidly dampen system oscillations and stabilize the closed-loop dynamics. Future research will focus on extending this approach to robust adaptive control designs capable of handling disturbances.

REFERENCES

[1] P. Kundur, *Power System Stability and Control*, McGraw-Hill, 1994.

[2] W. Dib, G. Kenné and F. Lamnabhi-Lagarrigue, An application of immersion and invariance to transient stability and voltage regulation of power systems with unknown mechanical power, *Proc. of the 48h IEEE Conference on Decision and Control (CDC) Held Jointly with 2009 28th Chinese Control Conference*, Shanghai, China, pp.7837-7842, 2009.

[3] W. Dib, R. Ortega, A. Astolfi and D. Hill, Improving transient stability of multi-machine power systems: Synchronization via immersion and invariance, *Proc. of American Control Conference*, San Francisco, CA, USA, 2011.

[4] M. O. Paul and E. P. Gerardo, Output feedback excitation control of synchronous generators, *International Journal of Robust and Nonlinear Control*, vol.14, pp.879-890, 2004.

[5] N. Jiang, X. Chen, T. Liu, B. Liu and Y. Jing, Nonlinear steam valve adaptive controller design for the power systems, *Intelligent Control and Automation*, vol.2, pp.31-37, 2011.

[6] Q. Lu, Y. Sun and S. Wei, *Nonlinear Control Systems and Power System Dynamics*, Kluwer Academic Publishers, Boston, 2001.

[7] L. Sun and J. Zhao, A new adaptive backstepping design of turbine main steam valve control, *Journal of Control Theory Applications*, vol.8, pp.425-428, 2010.

[8] B. Wang and Z. Mao, Nonlinear variable structure excitation and steam valving controllers for power system stability, *Journal of Control Theory Applications*, vol.7, pp.97-102, 2009.

[9] S. Xu and X. Hou, A family of robust adaptive excitation controllers for synchronous generators with steam valve via Hamiltonian function method, *Journal of Control Theory Applications*, vol.10, pp.11-18, 2012.

[10] J. Ma, Z. Xi, S. Mei and Q. Lu, Nonlinear stabilizing controller design for the steam-valving and excitation system based on Hamiltonian energy theory, *Proceedings of CESS*, vol.22, pp.83-93, 2002.

[11] Y. Guo, D. J. Hill and Y. Wang, Nonlinear decentralized control of large-scale power systems, *Automatica*, vol.36, pp.1275-1289, 2000.

[12] R. K. Aggarwal and B. W. Hogg, Control of dual-excitation generator using derivatives of rotor angle, *Proceedings of the Institution of Electrical Engineers*, vol.121, pp.1134-1140, 1974.

[13] B. Wang and W. Lin, Bounded control of dual-excited synchronous generator by using a passivity-based approach, *Proc. of the 8th World Congress on Intelligent Control and Automation*, Taipei, Taiwan, 2011.

[14] H. Chen, H. B. Ji, B. Wang and H. S. Xi, Coordinated passivation techniques for the dual-excited and stream-valving control of synchronous generators, *IEE Proc. of Control Theory Applications*, vol.149, pp.659-666, 2006.

[15] Y. Chang, C.-C. Wen, S.-W. Lin and Y.-C. Chen, Sliding mode control for the dual-excited and steam-valving control of synchronous generators, *Applied Mechanics and Materials*, vols.284-287, pp.2320-2324, 2013.

[16] Y. Chang and C.-C. Wen, Sliding mode control for the synchronous generators, *AISRN Applied Mathematics*, vol.2014, Article ID 256504, 2014.

[17] A. Kanchanahanathai, Immersion and invariance-based nonlinear dual-excitation and steam-valving control of synchronous generators, *International Transactions on Electrical Energy Systems*, vol.24, no.12, pp.1671-1687, 2014.
[18] A. Kanchanahanathai and A. Boonyaprapasorn, Nonlinear dual-excited and steam-valving control of synchronous generators via immersion and invariance, *Rangsit Journal of Arts and Sciences*, vol.3, no.2, pp.155-168, 2013.
[19] A. Kanchanahanathai, P. Konkhum and K. Wongsurith, A backstepping sliding mode dual-excitation and steam-valving control of synchronous generators, *International Reviews of Automatic Control*, vol.10, no.2, pp.159-167, 2017.
[20] A. Kanchanahanathai and E. Mujjalinvimut, Nonlinear disturbance observer-based backstepping control for a dual excitation and steam-valving system of synchronous generators with external disturbances, *International Journal of Innovative Computing, Information and Control*, vol.14, no.1, pp.111-126, 2018.
[21] Y.-H. Liu, Adaptive dynamic surface asymptotic tracking for a class of uncertain nonlinear systems, *International Journal of Robust, Nonlinear and Control*, vol.28, pp.1-13, 2017.
[22] E. Rashedi, H. Nezamabadi-pour and S. Saryazdi, GSA: A gravitational search algorithm, *Information Sciences*, vol.179, pp.2232-2248, 2009.
[23] E. Rashedi, E. Rashedi and H. Nezamabadi-pour, A comprehensive survey on gravitational search algorithm, *Swarm and Evolutionary Computation*, vol.41, pp.141-158, 2018.
[24] M. Krstic, I. Kanellakopoulos and P. V. Kokotivic, *Nonlinear and Adaptive Control Design*, John Willey & Sons, 1995.
[25] Z. Zho and C. Wang, Adaptive trajectory tracking control of output constrained multi-rotors systems, *IET Control Theory Applications*, vol.8, pp.1163-1174, 2014.

Author Biography

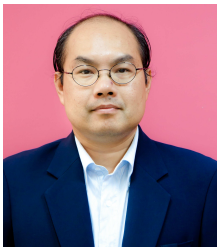

Adirak Kanchanaharuthai received Ph.D. degree in Systems and Control Engineering from Case Western Reserve University, Cleveland, OH, USA, in 2012. Currently, he is with Department of Electrical Engineering, Rangsit University, Thailand. His main research interests include power system dynamics, stability, and control, as well as applications of nonlinear control theory to power systems.

Pinit Ngamsom received Ph.D. degree in Mechanical Engineering from Oklahoma State University, USA in 2001. He is now with Department of Mechanical Engineering at Rangsit University, Thailand. His main research interests include robotics and control systems.

Kruawan Wongsurith received the M.Sc. degree in Chemistry from Srinakharinwirot University, Thailand, in 1994. She is currently a lecturer in the Faculty of Engineering at Kasem Bundit University, Thailand. Her main research interests include nonlinear dynamics and applications of control system design to chemistry process.